DEUTSCHES ELEKTRONEN-SYNCHROTRON DESY

DESY 84-111
November 1984

ON THE UNIQUE NUMERICAL SOLUTION OF MAXWELLIAN EIGENVALUE PROBLEMS IN THREE DIMENSIONS

by

T. Weiland

Deutsches Elektronen-Synchrotron DESY, Hamburg

ISSN 0418-9833

NOTKESTRASSE 85 · 2 HAMBURG 52

To be sure that your preprints are promptly included in the
HIGH ENERGY PHYSICS INDEX ,
send them to the following address (if possible by air mail) :

DESY
Bibliothek
Notkestrasse 85
2 Hamburg 52
Germany

DESY 84-111
November 1984

ISSN 0418-9833

On the unique numerical solution of Maxwellian Eigenvalue Problems in three dimensions

by

T. Weiland

LIST OF SYMBOLS

Z_o, Y_o	free space impedance, admittance $Z_oY_o = 1$, $Z_o = \sqrt{\mu_o/\epsilon_o}$
μ_o, ϵ_o	permeability, permittivity of vacuum
μ_r, ϵ_r	relative permeability, permittivity
μ, ϵ	permeability, permittivity, $\mu = \mu_r\mu_o$, $\epsilon = \epsilon_r \epsilon_o$
ω	circular frequency
c	speed of light in vacuum
$\vec{\underline{E}}$, $\vec{\underline{H}}$	vector of electric/magnetic field
$\vec{\underline{D}}$, $\vec{\underline{B}}$	vector of electric/magnetic flux density
$\vec{E},\vec{H},\vec{D},\vec{B},\vec{J}$	normalized vectors, e.g. $\vec{\underline{E}} = \vec{E}\sqrt{Z_o}\sin\omega t$, $\vec{\underline{H}} = \vec{H}\sqrt{Y_o}\cos\omega t$
$\vec{e}$, $\vec{h}$	vector holding all electric/magnetic field components in the grid
$\vec{d}$, $\vec{b}$	vector holding all electric/magnetic flux densities
G, $\tilde{G}$	grid, dual grid
M_u,M_v,M_w	index increments for linear numbering
u, v, w	orthogonal coordinates
D_A, $D_{\tilde{A}}$	diagonal matrix holding cell areas in G, $\tilde{G}$
D_s, $D_{\tilde{s}}$	diagonal matrix holding step sizes in G, $\tilde{G}$
D_v	diagonal matrix with volume of grid cells
D_ϵ , D_μ	diagonal matrix with permittivities/permeabilities
A_u,A_v,A_w	basic discretization matrix
C	discrete curl operator in grid space G
C^*	transpose of C = discrete curl operator in dual grid $\tilde{G}$
S	discrete div operator in grid space G
D_δ	Kronecker diagonal matrix with 1 on free space grid nodes, else 0

ABSTRACT

The numerical computation of eigensolutions of Maxwell's equations does not necessarily yield unique solutions - especially when applied to three dimensional problems. Thus an accurate calculation can become extremely difficult and the results uncertain.

This problem can be overcome by using a special finite difference method that solves all the four Maxwell equations in a consistent way, so that the properties of the differential equations and their solutions are still exhibited in the grid space for the corresponding matrix equations and their discrete solutions. By utilizing a simple combination of Maxwell's equations in the grid space we find a matrix representation with non-vanishing eigenvalues and thus unique solutions. This matrix equation corresponds to the wave equation in free space.

Numerical examples prove the stability and simplicity of the algorithm as well as the accuracy in comparison with measurements.

INTRODUCTION

We consider solutions of Maxwell's equations with harmonic time dependence. Thus we may write Maxwell's equations for loss free materials without any further restriction as:

$$\text{curl } \vec{H} = \frac{\omega}{c} \varepsilon_r \vec{E} \quad , \tag{1}$$

$$\text{curl } \vec{E} = \frac{\omega}{c} \mu_r \vec{H} \quad , \tag{2}$$

$$\text{div } \varepsilon_r \vec{E} = \rho \quad , \tag{3}$$

$$\text{div } \mu_r \vec{H} = 0 \quad . \tag{4}$$

For a given geometry, distribution of ε_r and μ_r and boundary conditions we are interested in eigensolutions of the above system for the lowest few eigenvalues. Practical examples for this problem can be found wherever rf-resonators are used that do not have higher symmetries. In this paper we focus on fully three dimensional problems - the two- and quasi two-dimensional cases can be considered to be solved[1].

Various numerical methods have been proposed in the last decade for discretizing the problem[2-4]. However, none of the algorithms has been free of severe numerical problems caused by a mixing of eigensolutions with trivial solutions ($\omega = 0$). This was especially true when three dimensional problems were attacked and the appearance of "ghost modes" left the judgement of whether a solution was correct or not to the user. This in fact is an unsatisfactory procedure.

The appearance of non-unique solutions is basically due to the fact that solving Maxwell's curl equations 1 and 2 combined as

$$\text{curl } \frac{1}{\mu_r} \text{curl } \vec{E} = \left(\frac{\omega}{c}\right)^2 \varepsilon_r \vec{E} \tag{5}$$

yields two distinct groups of solutions:

a) $\omega \equiv 0$, $\text{curl } \vec{E} = 0$, static fields
b) $\omega \neq 0$, resonant solutions.

The fact that there exist trivial ($\omega = 0$) solutions of equation 5 implies that the discretizised equation will have a matrix with vanishing eigenvalues. Thus discretizised solutions for $\omega \neq 0$ are not unique and are in general a mixture with all possible static fields.

When the metallic boundaries are simply connected, such fields can be caused only by real electric charges on non-conducting surfaces.

Analytically, the problem may be solved by imposing an additional constraint on the fields away from metallic boundaries:

$$\operatorname{div} \varepsilon_r \vec{E} = 0 \qquad (6)$$

This condition excludes all solutions with static content - for simply connected regions. The way of combining equations 6 and 5 is somewhat arbitrary. Using the "penalty parameter"[4]s one can write:

$$\operatorname{curl} \frac{1}{\mu_r} \operatorname{curl} \vec{E} - s \operatorname{grad} \operatorname{div} \varepsilon_r \vec{E} = \left(\frac{\omega}{c}\right)^2 \varepsilon_r \vec{E} \qquad (7)$$

By solving the above equations for various numerical values of s one finds solutions that do not depend on s and thus can be considered "good solutions". Since one has to undertake many computations and each one is extremely time consuming the situation remains unsatisfactory.
For $s = 1$, $\varepsilon_r = 1$ and $\mu_r = 1$ we obtain the wave equation:

$$\nabla^2 \vec{E} + \left(\frac{\omega}{c}\right)^2 \vec{E} = 0 \qquad (8)$$

This equation offers a simple way of avoiding static solutions. Since the constraint of equation 6 is incorporated, we expect only unique solutions when discretizising the wave equation. Though restricted to the case of the vacuum with metallic boundaries but without material insertions, this way promises unique numerical solutions for many realistic problems.

However, it has been found that the discretization of the wave equation can still yield "unphysical" solutions or "ghost modes"[3]. The reason for this is that not every numerical discretization method is consistent with Maxwell's equations in the sense that the analytical properties are transferred to the grid solutions. Thus severe difficulties arise when standard discretization methods are applied to Maxwell's vector field problems - especially when complicated boundary conditions are present.

In this paper we describe a consistent algorithm (FIT-method) that has been applied previousy to many field problems . This algorithm produces a matrix equation for each of the four Maxwell's equations. The combination of the matrix equations yields a symmetric operator having unique solutions in the grid space.

The key point of the method is that all four Maxwell's equations are discretizised in a consistent way: i.e. time harmonic fields that are source free in the real space also are source free in the grid space. Thus it is easy to eliminate all non time dependent field contents that cause non-unique solutions in other algorithms.

The method works in any orthonormal coordinate system and includes arbitrary distributions of permittive and permeable material in the region of solution.

THE METHOD

We use a topologically regular grid G in an orthonormal coordinate system (u, v, w) defined as:

$$G = \{(u_i, v_j, w_k) \in \mathbb{R}^3 \; ; \; u_1 \le u_i \le u_I, \; i = 1, \ldots, I \\ v_1 \le v_j \le v_J, \; j = 1, \ldots, J \\ w_1 \le w_k \le w_K, \; k = 1, \ldots, K \} \; . \qquad (9)$$

We use a linear numbering system for the grid nodes

$$n = 1 + (i - 1) \cdot M_u + (j - 1) \cdot M_v + (k - 1) \cdot M_w \qquad (10)$$

with $n = 1, \ldots, N \; ; \; N = I \cdot J \cdot K$

and $M_u = 1 \; , \; M_v = I \; , \; M_w = I \cdot J, \qquad (11)$

or any permutation of the latter three assignements. Figure 1 shows a sketch of such a topological grid.

We then have to allocate components of the unknown fields or vector potentials to the grid and we use the FIT algorithm[5,6] that allocates different components of the electric field to different locations in G as shown in Figure 2. This method also uses a dual grid $\tilde{G}$ in which the components of the magnetic field are assigned in the same way as the electric field is in G (for more details see references 5 and 6).

An approximate solution of Maxwell's equation may be obtained by evaluating the integrals along the circumference of each grid cell surface in first order approximation. Solving equ. 2 in integral form:

$$\oint \vec{E} \cdot d\vec{s} = \frac{\omega}{c} \iint \vec{B} \cdot d\vec{A} \qquad (12)$$

over the cell surface perpendicular to the w-axis shown in fig. 2 yields:

$$(u_{i+1} - u_i) \cdot (E_{u,n} - E_{u,n+M_v}) + (v_{j+1} - v_j) \cdot (E_{v,n+M_u} - E_{v,n})$$

$$= \frac{\omega}{c}(u_{i+1} - u_i) \cdot (v_{j+1} - v_j) \cdot B_{w,n} \qquad (13)$$

In order to get more insight into the algebraic structure of this algorithm we must introduce a few definitions.
Putting all unknown components of the fields into column vectors yields:

$$\vec{e} = (E_{u_1}, E_{u_2}, \ldots, E_{uN}, E_{v_1} \ldots E_{wN})^* \qquad (14)$$

$$\vec{b} = (B_{u_1}, B_{u_2}, \ldots, B_{uN}, B_{v_1} \ldots B_{wN})^* \qquad (15)$$

The mesh step sizes occuring in equ. 13 are put into a diagonal matrix

$$D_s = \text{Diag}\,\{(u_2 - u_1), \ldots, (u_I - u_{I-1}), 0, (u_2 - u_1), \ldots, (w_K - w_{K-1}), 0\} \qquad (16)$$

each element of which is holding the step size value for the electric field component along that grid element.

Similarly we can define a diagonal matrix D_A holding all the cell surface areas that belong to the components of the magnetic field (see figure 1).
Finally, we define the band matrix:

A_u =

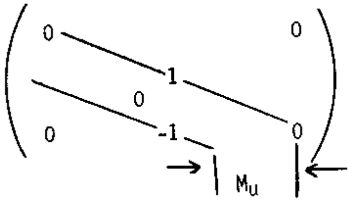

(17)

which enables us to write the matrix equation representing equ. 13 at all grid nodes in a simple algebraic matrix occuring in equ. 18.

The matrix A_u has only two bands at a distance given by the definition of the linear numbering system, equs. 10 and 11.

We now can write down the analogue of Maxwell's equation (2) in the grid space as:

$$\begin{pmatrix} 0 & A_w^* & -A_v^* \\ -A_w^* & 0 & A_u^* \\ A_v^* & -A_u^* & 0 \end{pmatrix} \cdot D_s \vec{e} = \left(\frac{\omega}{c}\right) D_A \vec{b} \qquad (18)$$

In order to introduce the distribution of material in the grid space we define diagonal matrices correlating the field strengths and the flux densities in the grid space:

$$\vec{b} = D_\mu \vec{h} \quad \longleftrightarrow \quad \vec{B} = \mu \cdot \vec{H} \qquad (19)$$

$$\vec{d} = D_\varepsilon \vec{e} \quad \longleftrightarrow \quad \vec{D} = \varepsilon \cdot \vec{E} \qquad (20)$$

Performing the same procedure for the first Maxwell equation and replacing the grid quantities in G by those in the dual grid $\tilde{G}$ (see for more details ref. 5 and 6) we obtain

$$\begin{pmatrix} 0 & -A_w & A_v \\ A_w & 0 & -A_u \\ -A_v & A_u & 0 \end{pmatrix} \cdot D_{\tilde{s}} D_\mu^{-1} \vec{b} = \left(\frac{\omega}{c}\right) D_{\tilde{A}} D_\varepsilon \vec{e} \qquad (21)$$

These equations also contain the rows and columns that belong to already known components e.g. those vanishing due to boundary conditions. This is done in order to maintain the simple algebraic structure of the matrices. However, in a computer code one can always compress the equations in such a way that they only have real unknowns to work on.
Using the abbreviation C for the algebraic curl operator

$$C = \begin{pmatrix} 0 & -A_w & A_v \\ A_w & 0 & -A_u \\ -A_v & A_u & 0 \end{pmatrix} \qquad (22)$$

we can combine equations 18 and 21 to give:

$$\left(\frac{\omega}{c}\right)^2 \cdot D_\varepsilon \cdot D_{\tilde{A}} \cdot \vec{e} = C\, D_\mu^{-1} D_{\tilde{s}} D_A^{-1} C^* D_s \vec{e} \qquad (23)$$

This is an algebraic eigenvalue equation for the unknown electric field components with an asymmetric matrix. However, we find that the system matrix is topologically symmetric: In the case of a uniform medium and a regularly spaced grid we find:

$$(D_\varepsilon = D_\mu = D_A = D_{\tilde{A}} = D_s = D_{\tilde{s}} = \text{unit matrix}):$$

$$\left(\frac{\omega}{c}\right)^2 \cdot \vec{e} = CC^* \vec{e} \qquad (24)$$

In order to convert the algorithm into a symmetric form in the general case we must perform a diagonal transformation, which physically replaces the field strength by the local density of the stored energy:

$$\vec{e}\,' = (D_\varepsilon \, D_{\tilde{A}} \, D_S)^{1/2} \, \vec{e} \tag{25}$$

Now, instead of equ. 23 we obtain:

$$(\tfrac{\omega}{c})^2 \, \vec{e}\,' = (\tilde{D} \, C \, D) \, (\tilde{D} \, C \, D)^* \, \vec{e}\,' \tag{26}$$

using the abbreviation

$$D = D_\mu^{-1/2} \, D_{\tilde{S}}^{1/2} \, D_A^{-1/2} \tag{27}$$

$$\tilde{D} = D_\varepsilon^{-1/2} \, D_S^{1/2} \, D_{\tilde{A}}^{-1/2} \tag{28}$$

Equation 26 is finally symmetric and has some remarkable properties:

- C is a canonical matrix with elements only taking values +1, -1 or 0.
- All information about mesh step sizes and material distribution is held in diagonal matrices.
- The matrix is symmetric and thus we have only real values for ω^2.

However, as mentioned earlier, the eigenvalue equation not only has non-trivial solutions but also describes static solutions with $\omega \equiv 0$. When the metallic boundaries are simply connected, such fields can be caused only by real electric charges on non-conducting surfaces. Thus we can avoid these solutions by imposing the above condition on equation 26. To do this we discretisize the equation

$$\text{div } \varepsilon_r \, \vec{E} = \rho \tag{29}$$

Defining $\vec{q}$ as the vector of dimension N holding the values of the charges on each grid node we find that the discretisized form of equation 29 reads simply as:

$$(A_u \,\vdots\, A_v \,\vdots\, A_w) \cdot D_\varepsilon \, D_{\tilde{A}} \, \vec{e} = \vec{q} \tag{30}$$

This equation can be easily understood using figure 3. In order to construct a 3N by 3N matrix equation from equ. 30 and to combine it with equ. 26 we define another diagonal matrix

$$D_V = \text{Diag } \{V_1, \ldots, V_n, V_1, \ldots, V_n, V_1, \ldots V_n\} \tag{31}$$

that holds all volume elements three times, one for each component.

The matrix $S = (A_u \,\vdots\, A_v \,\vdots\, A_w)$ of order N x 3N in equ. 30 is used to construct a symmetric 3N by 3N equation for the transformed field components:

$$\tilde{D}^{-1} \, S^* \, D_V^{-1} \, S \, \tilde{D}^{-1} \, \vec{e}\,' = \vec{q}\,' \, . \tag{32}$$

We now define a Kronecker matrix D_δ with 1 for mesh points that do not lie on a metallic boundary and with a zero for all nodes on a metallic boundary. Then we can transform equation 32 into

$$D_\delta \, \tilde{D}^{-1} \, S^* \, D_V^{-1} \, S \, \tilde{D}^{-1} \, D_\delta \, \vec{e}\,' = 0 \tag{33}$$

The latter equation explicitly imposes the condition on the electric field that there are no charges in free space and thus excludes static solutions. Note that this equation is equivalent to the replacement:

$$\text{grad div } \varepsilon_r \, \vec{E} \quad \longleftrightarrow \quad D_\delta \, \tilde{D}^{-1} \, S^* \, D_V^{-1} \, S \, \tilde{D}^{-1} \, D_\delta \cdot \vec{e}\,' \tag{34}$$

Finally we combine the discrete curl-curl operator and the source equation to give:

$$[(\tilde{D} C D) \cdot (\tilde{D} C D)^* + (D_V^{-1/2} S \, \tilde{D}^{-1} \, D_\delta)^* \cdot (D_V^{-1/2} S \, \tilde{D}^{-1} \, D_\delta)] \, \vec{e}\,' = (\tfrac{\omega}{c})^2 \, \vec{e}\,' \tag{35}$$

Solutions of this equation fulfill the condition $\omega^2 \varepsilon \mathbb{R}$, and form a complete basis. In fact, it can be shown (Appendix) that $\omega^2 \geq 0$ and thus that all frequencies ω are real.

The discrete operator has the following remarkable properties:

1) The global structure is given by

$$B \, \vec{e}\,' = (\tfrac{\omega}{c})^2 \, \vec{e}\,' \quad , \qquad B = \begin{pmatrix} B_{uu} & B_{uv} & B_{uw} \\ B_{uv}^* & B_{vv} & B_{vw} \\ B_{uw}^* & B_{vw}^* & B_{ww} \end{pmatrix}$$

2) The matrix is real and symmetric
3) The matrix is semi definite.
   (Though not strictly proved, it is obvious from the above that the matrix is in fact positive definite for simply connected regions.)
4) The matrix is composed of simple products and sums of canonical operators. Mesh step sizes and material properties are kept in separate diagonal matrices.
5) All logical connections are based on one single difference operator matrix with two bands: see equ. 17.

One other very interesting property of the final matrix is that for the simplified cases of free space and homogeneous media all elements in the coupling matrices B_{uv}, B_{uv} and B_{vw} vanish. Thus we have three independent equations that are coupled only at the boundary or at any location where the material property changes. In the case of free space the diagonal main matrices B_{uu}, B_{vv} and B_{ww} turn into the well-known discrete ∇^2 operator with a 6 on the diagonal and six times -1 on side diagonals.

This way of deriving the final matrix appears to be rather complicated. However, a direct discretization for the general case of equ. 5 seems to be much more complicated. The way described here needs only very basic operations since the final matrix is composed of a number of rather simple matrices. Last but not least, this method guarantees that there exists only physical and non-trivial solutions.

APPLICATION

A preliminary version of a three dimensional computer program has been prepared. The code allows for arbitrarily shaped structures with material insertions of permittive and/or permeable material. The examples presented here serve only as a proof of principle.

We first consider a cylindrically symmetric cavity with beam tubes as shown in figure 4. Figure 5 shows the representation of this cavity on a 41x41x41 grid. For the actual calculation, however, we use only one eighth and make use of the symmetry as shown in figure 6. Thus one has to run the code several times for the same geometry but with different boundary conditions on the planes of symmetry. This example has been chosen since it is possible to calculate the eigenfrequencies quite accurately with the 2D-code URMEL[7] (that makes use of the cylindrical symmetry and uses only a 2D grid). Table I shows the lowest modes found with both codes.

The URMEL[7] results are obtained for a plane grid of 5000 nodes giving a relative accuracy of 10^{-4}. Azimuthal mode numbers up to quadrupole (m = 0, 1, 2) were used.

Table I

Lowest modes in a cylindrical cavity with side tubes found using the 2D-code URMEL and by the three dimensional calculation.

	f/MHz		
Mode Type (notation see /7/)	URMEL N_2 = 5000	3D-calculation $N_3 = 21^3 = 9261$	error
TMØ-EE-1	116.53	116.76	$1.7 \cdot 10^{-3}$
1-ME-1	168.23	168.30	$4.2 \cdot 10^{-4}$
1-EE-1	179.14	179.24	$5.6 \cdot 10^{-4}$
TMØ-ME-1	190.76	190.71	$2.6 \cdot 10^{-4}$
2-ME-1	208.67	208.87	$9.6 \cdot 10^{-4}$
1-ME-2	225.97	226.30	$1.5 \cdot 10^{-3}$
2-EE-1	244.02	243.97	$2.0 \cdot 10^{-4}$

For comparison with some measured results we use the cavity shown in figure 7: a rectangular cavity with a rectangular post in the center. The two lowest modes have been measured[8] and table II shows the comparison with calculated data.

Table II

Lowest modes in a three dimensional rectangular cavity as measured and calculated (only one quarter was used in the calculation with $N_3 = 12 \cdot 16 \cdot 12 = 2304$).

Mode #	calculated frequency/MHz	measured frequency/MHz	error
1	17.09	17.39	$1.8 \cdot 10^{-2}$
2	45.09	45.06	$7.0 \cdot 10^{-4}$

As an example for a cavity with a dielectric insert we use the rectangular cavity loaded by a teflon tube[9] as shown in figure 8. Measured and calculated results agree very well as can be seen in table III.

Table III

Measured and calculated lowest resonant frequencies of a dielectric loaded (teflon tube) rectangular cavity (see figure 8).

	f/MHz		
	measured	calculated $N_3 = 690$	calculated $N_3 = 3185$
with dielectric tube	1258	1255	1256
without dielectric tube	1319	1310	1319

THE COMPUTER PROGRAM

A preliminary computer program has been prepared that can handle up to 20.000 nodes on an IBM 3081 using about 30 minutes cpu time for the ten lowest modes. The cpu time scales as $N^{1.5}$ with N as the total number of mesh points, see figure 9. This code is part of a family of 3D-codes and shares input and output facilities with other programs.

A joint effort between Los Alamos National Laboratory, Kernforschungsanlage Jülich and DESY has been started in order to prepare a much more user friendly and a much faster code within the near future.

SUMMARY

A numerical discretization method is described that enables the calculation of resonant modes in three-dimensional cavities of arbitrary shape with arbitrarily shaped insertions of material. The algorithm has only unique solutions and guarantees that no mixture with static fields occurs.

Though, only a preliminary version, the computer code can handle up to 20.000 grid nodes on an IBM 3081 using about 30 minutes cpu time for the ten lowest modes. This already enables the investigation of many basic rf-cavity problems.

ACKNOWLEDGEMENTS

The author wishes to thank D. Barber and R. Klatt for careful reading of the manuscript and for many useful hints. Also thanks are due to B. Dwersteg for doing the measurements of the dielectric cavity and due to R.K. Cooper who made available to me the measurements performed at Los Alamos National Laboratory.

LITERATURE

1. T. Weiland, "Design of r.f. cavities", DESY M-83-22 and Proceedings of the 1th Conference on Computing in Accelerator Design and Operation, Berlin, September 20-23, 1983

2. H. Albani and M. Bernardi, "A numerical method on the discretization of Maxwell's equations in integral form", IEEE, MTT22 (1974), 446-449

3. W. Wilhelm, "CAVIT and CAV3D - Computer Programs for rf-cavities with constant cross section or any three dimensional form", Particle Accelerator 12 (1982), p. 139

4. M. Hara, T. Wada, A. Toyanna, F. Kikuchi, "Calculation of RF Electromagnetic Feld by Finite Element Method", Scientific Papers of the Institute of Physical and Chemical Research 75 (1982), 143-175

5. T. Weiland, "A Discretization Method for the Solution of Maxwell's Equations for Six-Component Fields", AEÜ 31 (1977), p. 116-120

6. T. Weiland, "On the Numerical Solution of Maxwell's Equations and Applications in the Field of Accelerator Physics", Particle Accelerator 15 (1984), pp. 245-292

7. T. Weiland, "On the Computation of Resonant Modes in Cylindrically Symmetric Cavities", NIM 216 (1983), p. 329-348

8. These measurements have been performed by the rf-group in AT-division, Los Alamos National Laboratory, (results were scaled from inches to meters)

9. These measurements were performed by B. Dwersteg, DESY

APPENDIX

We rewrite equations 18 and 19 using 22 as

$$C^* D_S \vec{e} = \frac{\omega}{c} D_A \vec{b} \quad , \qquad \text{A1}$$

$$C D_{\tilde{S}} D_\mu^{-1} \vec{b} = \frac{\omega}{c} D_\varepsilon D_{\tilde{A}} \vec{e} \quad . \qquad \text{A2}$$

With the formal equations:

$$\vec{b} = D_\mu \vec{h} \quad , \quad k = \omega/c \qquad \text{A3}$$

we find

$$C^* D_S \vec{e} = k D_A D_\mu \vec{h} \quad , \qquad \text{A4}$$

$$C D_{\tilde{S}} \vec{h} = k D_{\tilde{A}} D_\varepsilon \vec{e} \quad . \qquad \text{A5}$$

We perform the same transformation as equ. 25 but also for the magnetic field:

$$\vec{e}' = (D_\varepsilon D_{\tilde{A}} D_S)^{1/2} \vec{e} \quad , \qquad \text{A6}$$

$$\vec{h}' = (D_\mu D_A D_{\tilde{S}})^{1/2} \vec{h} \quad . \qquad \text{A7}$$

and obtain

$$C^* D_S^{1/2} D_\varepsilon^{-1/2} D_{\tilde{A}}^{-1/2} \vec{e}' = D_A^{1/2} D_\mu^{1/2} D_{\tilde{S}}^{-1/2} \vec{h}' \quad , \qquad \text{A8}$$

$$C D_{\tilde{S}}^{1/2} D_\mu^{-1/2} D_A^{-1/2} \vec{h}' = k D_{\tilde{A}}^{1/2} D_\varepsilon^{1/2} D_S^{-1/2} \vec{e}' \quad . \qquad \text{A9}$$

Or with the abbreviation of equ. 27 and 28:

$$C^* \tilde{D} \vec{e} = k D^{-1} \vec{h}' \quad , \qquad \text{A10}$$

$$C D \vec{h} = k \tilde{D}^{-1} \vec{e}' \quad . \qquad \text{A11}$$

We multiply equ. A10 by D from the left and equ. A11 by $\tilde{D}$, we put h' and e' into one vector and find:

$$\begin{pmatrix} 0 & D C^* \tilde{D} \\ \tilde{D} C D & 0 \end{pmatrix} \begin{pmatrix} \vec{h}' \\ \vec{e}' \end{pmatrix} = k \begin{pmatrix} \vec{h}' \\ \vec{e}' \end{pmatrix} \qquad \text{A12}$$

The matrix of the eigenvalue problem in k is real and symmetric. Thus k is real and k^2 positive, i.e. equ. 35 has a semi positively defined matrix.

FIGURE CAPTIONS

Figure 1: Topologically regular grid in three dimensions.

Figure 2: The allocation of unknown field components in the grid.

Figure 3: Six electric field components contributing to the charge q_n on node number n.

Figure 4: Cylindrical cavity with beam tubes.

Figure 5: Mesh representation of the cylindrical cavity in a 41x41x41 grid.

Figure 6: One eighth of the cylindrical cavity used for the calculation.

Figure 7: Simple rectangular cavity with metallic post.

Figure 8: Rectangular cavity loaded with a dielectric tube.

Figure 9: cpu time T on an IBM 3081 D in seconds as function for number of nodes.

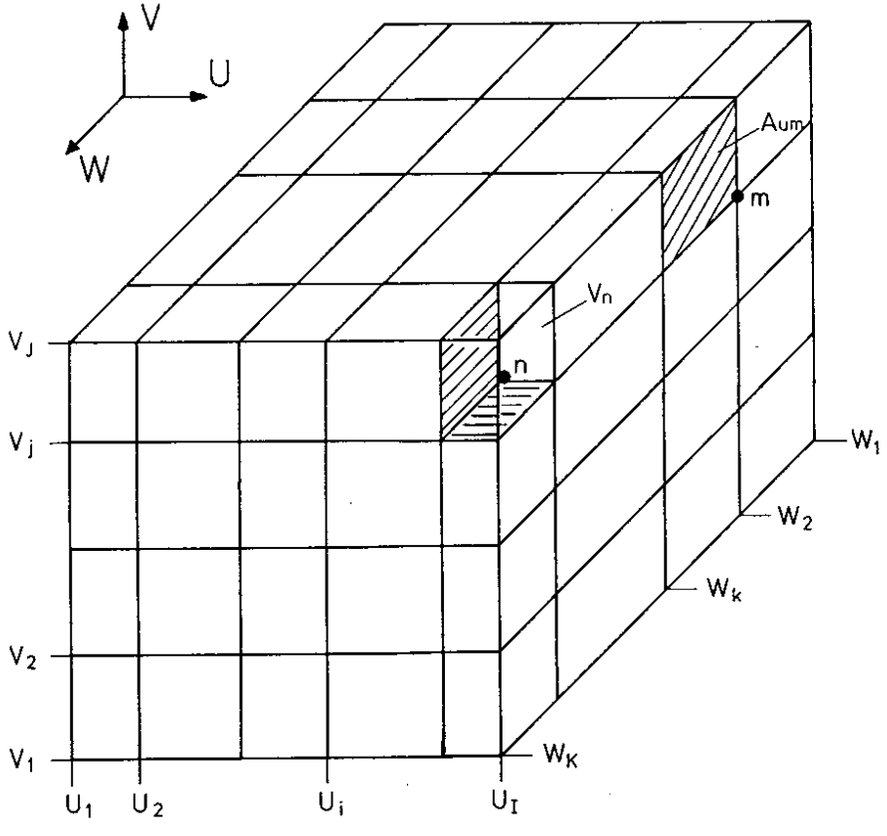

Figure 1: Topologically regular grid in three dimensions.

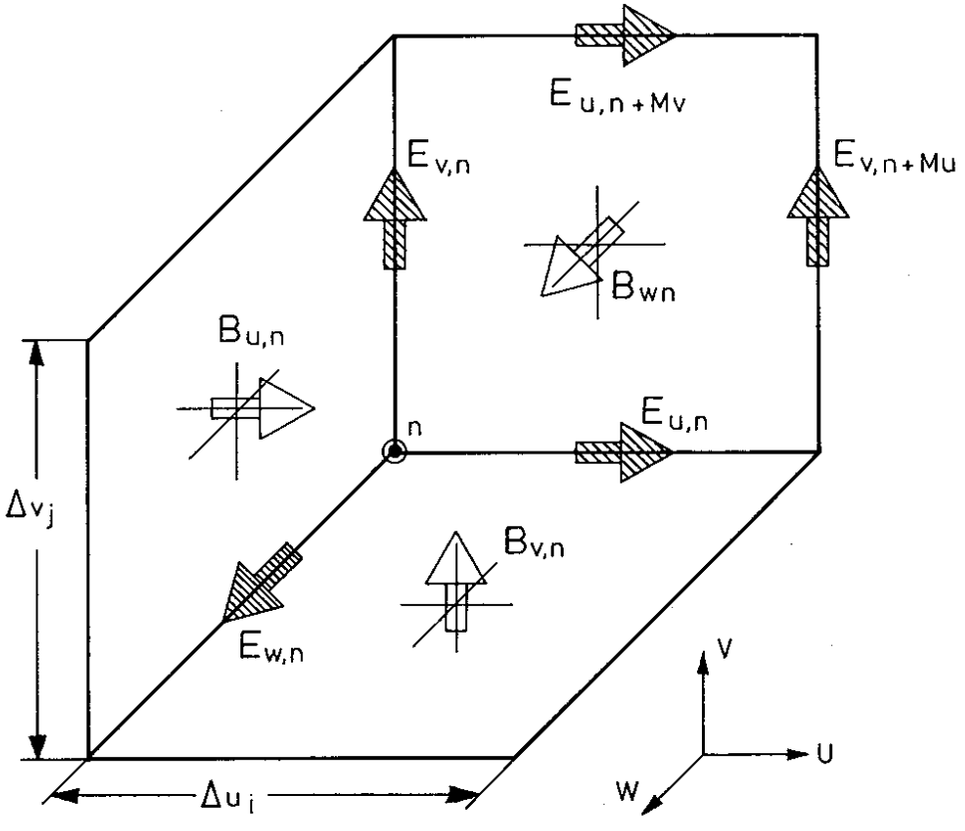

Figure 2: The allocation of unknown field components in the grid.

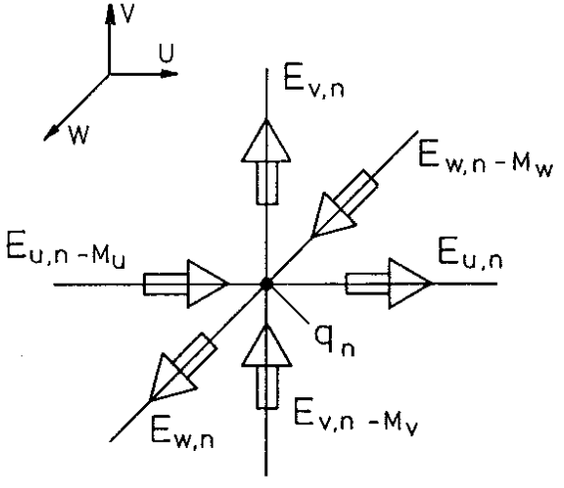

Figure 3: Six electric field components contributing to the charge q_n on node number n.

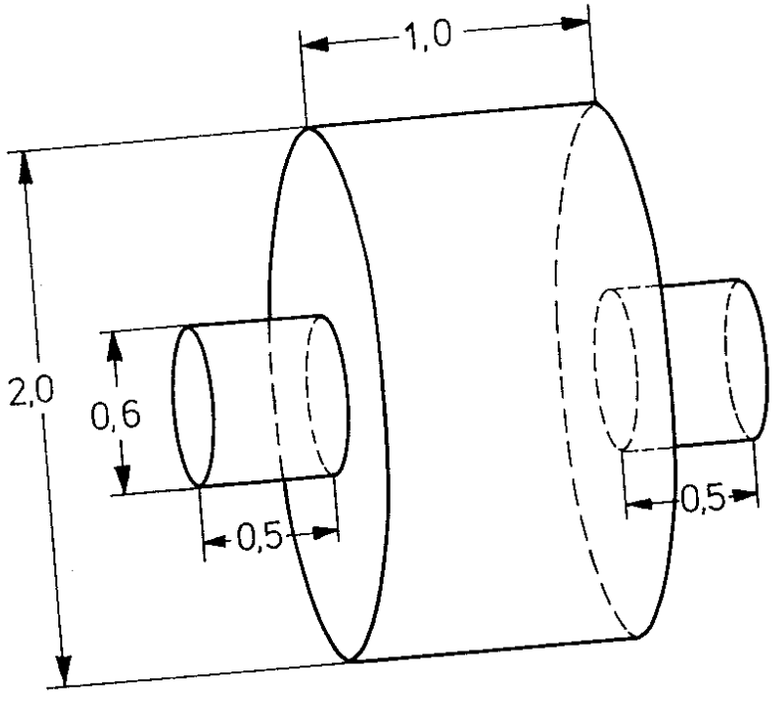

Figure 4: Cylindrical cavity with beam tubes.

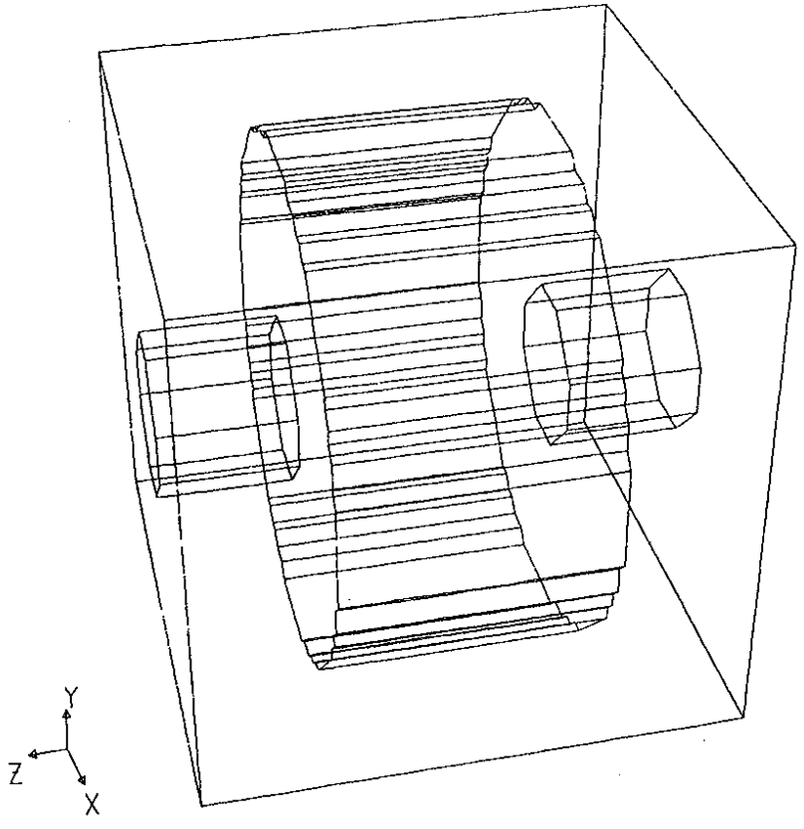

Figure 5: Mesh representation of the cylindrical cavity in a 41x41x41 grid.

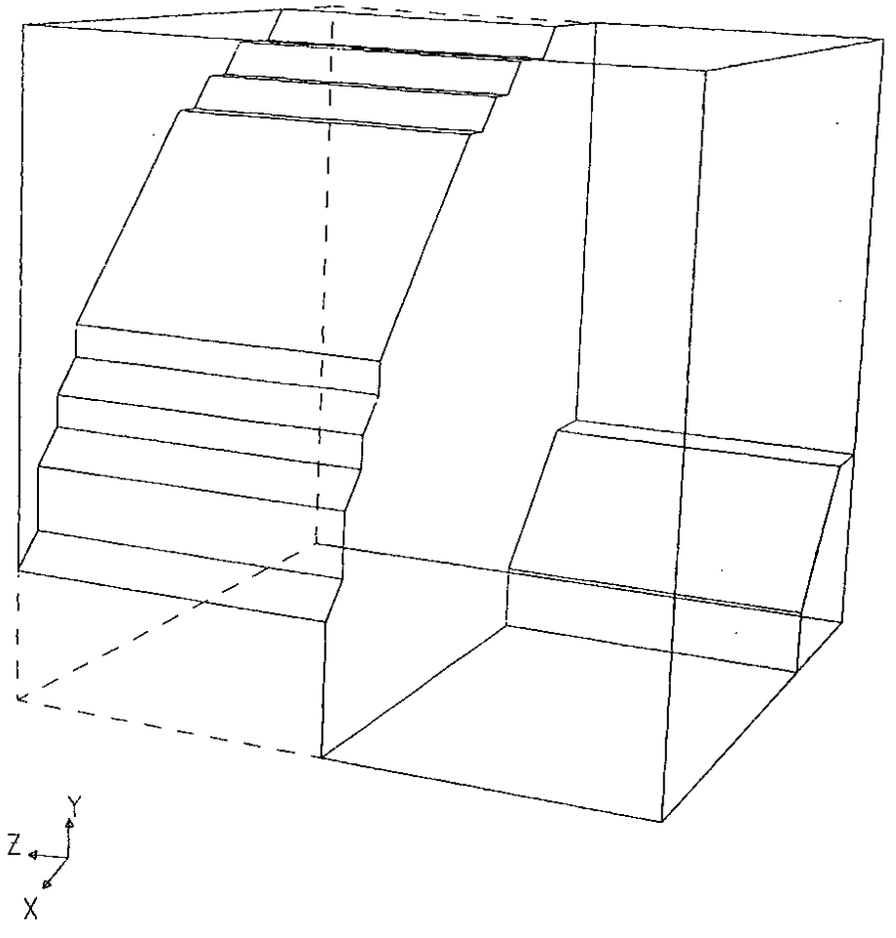

Figure 6: One eighth of the cylindrical cavity used for the calculation.

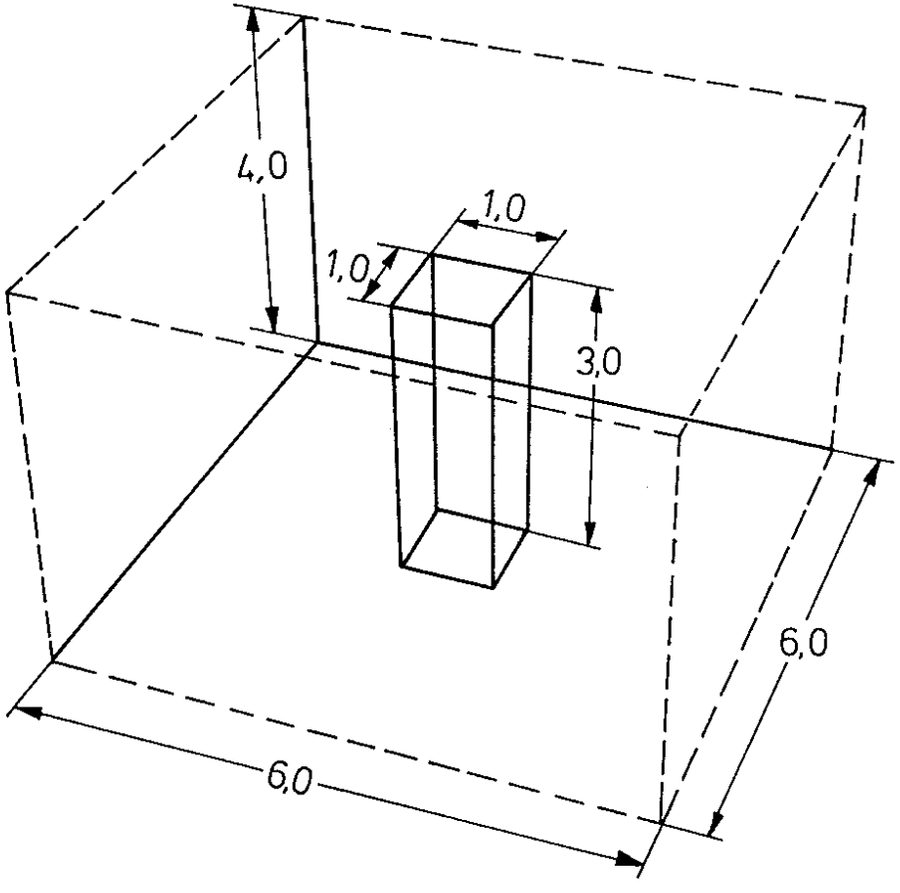

Fig. 7: Simple rectangular cavity with metallic post.

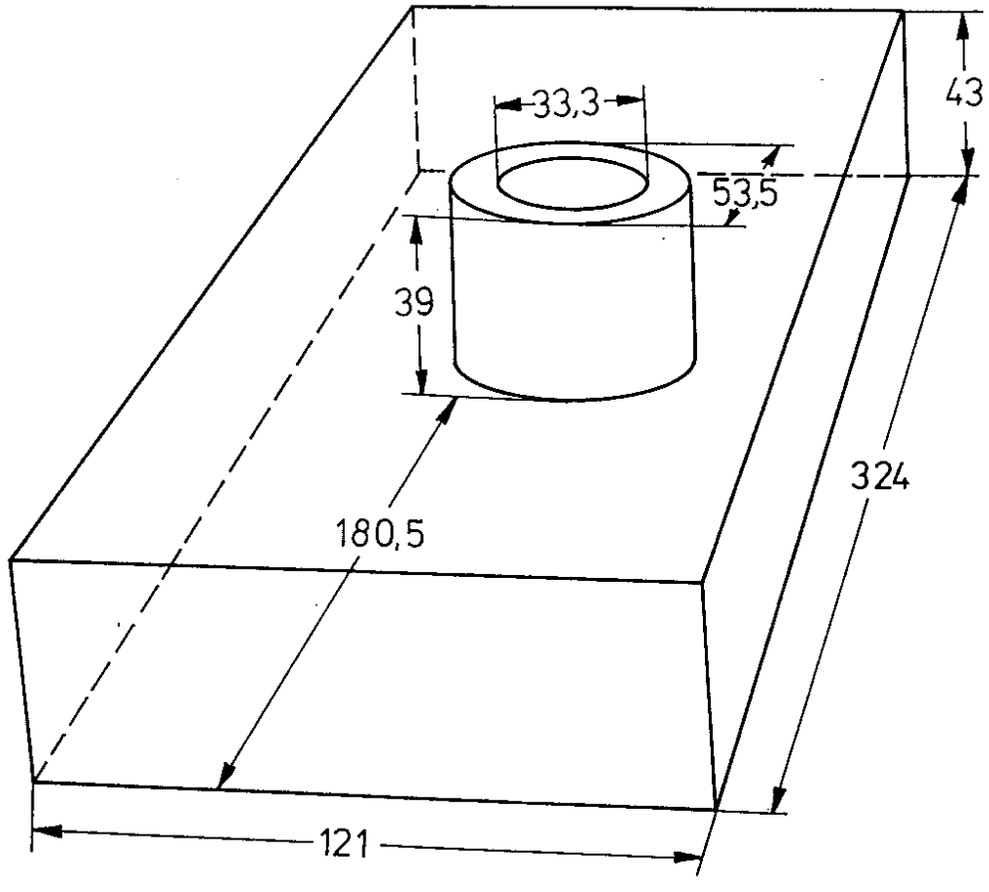

Fig. 8: Rectangular cavity loaded with a dielectric tube.

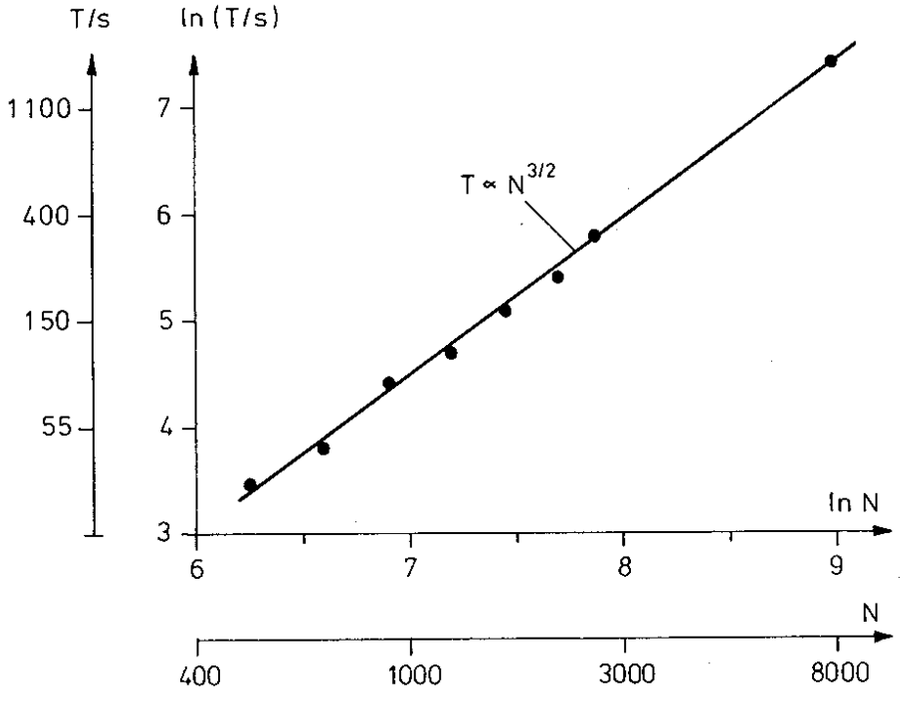

Figure 9: cpu time T on an IBM 3081 D in seconds as function for number of nodes.